Hindawi
Journal of Sensors
Volume 2021, Article ID 6625780, 16 pages
https://doi.org/10.1155/2021/6625780

Research Article

Elucidating the Capabilities of Mirrorless Large Core Bundled Plastic Fiber Optic Displacement Sensor for Paracetamol Detection

Mohd Zamani Zulkifli,[1] **Muhammad Fadhli Mohd Azri**,[1] **Muhammad Khudhori Mohd Yusof**,[1] **Saiful Arifin Shafiee**,[2] **Awis Sukarni Mohmad Sabere**,[3] **Lau Kuen Yao**,[4] **Sani Amril Samsudin**,[5] **Muhammad Syahril Bahari**,[6] **and Moh Yasin**[7]

[1]*Department of Physics, Kulliyyah of Science, International Islamic University Malaysia, Bandar Indera Mahkota, 25200 Kuantan, Pahang, Malaysia*
[2]*Department of Chemistry, Kulliyyah of Science, International Islamic University Malaysia, Bandar Indera Mahkota, 25200 Kuantan, Pahang, Malaysia*
[3]*Department of Pharmaceutical Chemistry, Kulliyyah of Pharmacy, International Islamic University Malaysia, Bandar Indera Mahkota, 25200 Kuantan, Pahang, Malaysia*
[4]*Department of Electronics and Nanoengineering, Tietotie 3, Aalto University, 02150 Espoo, Finland*
[5]*School of Chemical and Energy Engineering, Faculty of Engineering, Universiti Teknologi Malaysia (UTM), 81310 Johor Bahru, Johor, Malaysia*
[6]*Faculty of Mechanical Engineering Technology, Pauh Putra Campus, Universiti Malaysia Perlis (UniMAP), 02600 Arau, Perlis, Malaysia*
[7]*Faculty of Science and Technology, Department of Physics, Airlangga University, Surabaya, Indonesia*

Correspondence should be addressed to Mohd Zamani Zulkifli; mzz@iium.edu.my and Moh Yasin; yasin@fst.unair.ac.id

Received 1 December 2020; Revised 10 May 2021; Accepted 8 June 2021; Published 5 July 2021

Academic Editor: Bruno C. Janegitz

A simple mirrorless plastic optical fiber displacement sensor was used to determine the concentration of paracetamol (PCM) in an aqueous solution. Paracetamol concentrations between 5 and 45 ppm were tested by the proposed sensor. With a mirror, the substantial sensitivity observed by an output power changed against displacement of 0.0403 mW/μm for the front slope and 0.023 mW/μm for the back slope with linearities of more than 99%. On the other hand, nonmirror reflector showed a sensitivity of 0.0006 mW/μm for the front slope and 0.0002 mW/μm for the back slope for the case of a red reflector and a sensitivity of 0.0007 mW/μm and 0.0003 mW/μm for the front and the back slope, respectively, for the case of a white reflector. The sensor sensitivity for the red and white coloured papers, which were used as the nonmirror reflectors and the mirror reflector itself against changing PCM concentrations, was 0.0004 mW/ppm, 0.0008 mW/ppm, and 0.02 mW/ppm, respectively. The experimental results indicated that the sensor was not only able to detect and measure the concentration of PCM in aqueous solutions but was also very stable with the additional advantages of a cost-effective and practical design that is highly beneficial for real-world sensing applications.

1. Introduction

Acetaminophen, or more typically known as paracetamol (PCM), is one of the most commonly used and important antipyretic and anodyne pharmaceutical drugs in the world [1]. The applications of PCM are numerous, ranging from being used to help treat fevers to reducing coughing, chills, backache, sore muscles, toothache, severe pain, and even

migraines [2–4]. At medicinal doses, PCM is very safe and has no dangerous repercussions [5]. However, an overdose of PCM can lead to toxic metabolite accumulation that could cause severe consequences and side effects such as kidney and liver damage [6]. By itself, PCM typically does not pose any side effects to the consumers except for those who may have developed hypersensitivity or drug overdose which could result in nephrotoxicity, hepatotoxicity, or even renal failure due to the formation of toxic metabolites [7, 8]. While the chances of such side-effects are minor, they cannot be disregarded; to date, there have been more than 100,000 emergency phone calls, 56,000 emergency room visits, 2,600 hospitalisations, and 458 deaths related to acute liver failures due to PCM over dose per year in the US alone. This brings about a startling conclusion that PCM overdose occurrences are more common in comparison to the overdose of any other pharmaceutical compounds in the US [9]. In Australia, PCM overdose cases were reported at alarming rates which may be a result of public misconceptions on the safety of PCM, leading to its misuse and subsequently accidental overdose [10]. There have even been reports of rare situations in by Bourdeaux and Bewley of death from PCM overdose despite treating the patient with N-acetylcysteine [11]. Altogether, these incidences build a very strong case that PCM poisoning is not to be taken lightly. Further complications arise when taking into consideration that PCM and its chemical analogues can also easily accumulate in aquatic environments and in fact have been detected in surface water, wastewater, and drinking water in many parts of the world [12]. These contaminants originate from multiple sources including consumer use and disposal, hospital drug waste, and pharmaceutical manufacturing facilities [13–15]. Although the concentrations of PCM in water bodies range within nanograms to micrograms per liter, these biologically active drugs may still affect the sensitive aquatic organisms despite their very low concentrations [16]. Various health effects on aquatic organisms have been reported from exposure to even low levels of PCM which include acute and chronic damages, inhibition of cell growth, and behavioral alterations.

As a result of this, the development of simple and accurate methods to detect PCM constituents is crucial because towards regulating drug safety that affects the public health. In recent years, various types of sensors for the detection of PCM have been developed, including those based on electrochemical sensing [1, 17–20], ultraviolet and mass spectrometric detection [5], chemiluminescence detection [21, 22], sequential injection chromatographic determination [13], and fluorometric sequential injection analysis (SIA) optosensing [14]. However, all these methods require lengthy predetection extraction and long-running processes which are cumbersome when it comes to testing large amounts of samples for the presence of PCM, especially at healthcare centers. In light of these limitations, sensing application using optical fibers has recently becoming increasingly popular. Optical fibers have long been the mainstay of communication domain, but its applications in sensing have also been recently exploited with researchers discovering that these sensors could not only be used to detect many of physical parameters of traditional sensors but also with great sensitivity and efficiency. Many optical fiber sensors have been demonstrated including those used for the detection of liquid solution concentrations such as glucose [15], calcium [23], honey [24], cholesterol [25], formaldehyde [26], and sodium chloride [27]. Furthermore, plastic optical fiber displacement sensors (POFDS) have shown significant promise due to its various advantages such as being resistant to electromagnetic interference, consistent, highly sensitive, and operable in any situation [15]. These, combined with its low cost, make POFDS a very suitable tool for chemical sensing. POFDS have grown to be one of the most versatile sensors in accordance to its application [23]. These sensors could be used to measure various physical and chemical parameters such as vibration, temperature, and pressure as well as pH levels, concentration, density, and even the refractive index of liquids. Table 1 shows a basic analytical parameters for comparison between the sensors reported [28–32].

Table 1: Fiber optic sensor and its applications.

Application	Parameters
Physical sensors	Temperature, humidity, pressure, width, thickness, etc.
Chemical sensors	pH calculation, analyse gas content, concentration of solution, etc.
Biomedical sensors	Blood flow measurement, glucose content, etc.

With these great advantages, developing a simple and accurate approach using POFDS to detect PCM would be highly desirable by pharmaceutical industries to realise detection that is fast, simple, and inexpensive but with good accuracy. The main goal of this work is to develop a simple mirrorless POFDS to detect the presence of PCM with better precision and sensitivity. The principle behind the POFDS to determine PCM concentrations is based on a very simple yet highly sensitive and accurate detection scheme which is by measuring the intensity of the reflected laser light from the target surface placed at the bottom of the samples as modulated intensity dependent sensors detect the amplification of the light that has travelled between the sensor head and the target surface. This proposed technique is simple and reliable as well as time and cost-effective as compared to existing pharmaceutical sensors.

2. Principle of Bundled Displacement Sensor

In order to more easily analyse the principle behind the fiber bundle, a number of assumptions are made [33]:

(1) The fiber bundles are modelled as one transmitting fiber (TF) and one receiving fiber (RF) that are close to each other with no gap between both fibers

(2) Both fibers are assumed to have a same cross section S_a with radius ω_a (see Figure 1(b))

(3) The light from TF is characterized as a symmetrical cone with an angle of divergence θ_a and the origin 0 positioned at z_a inside the TF

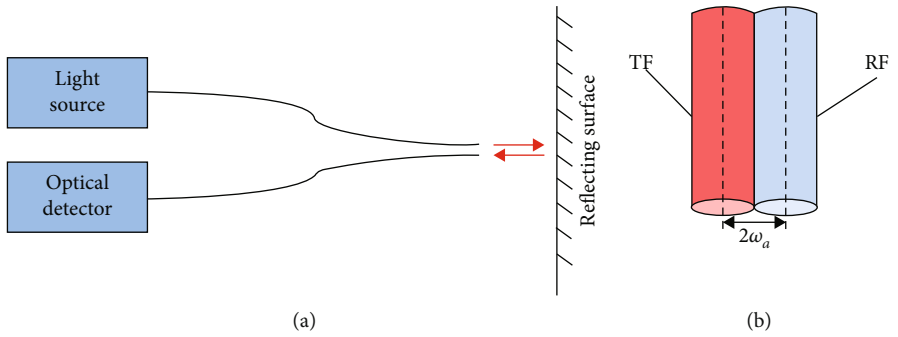

Figure 1: (a) Basic configuration of fiber bundle displacement sensor. (b) Side view of TF and RF in the context of the mathematical simulation.

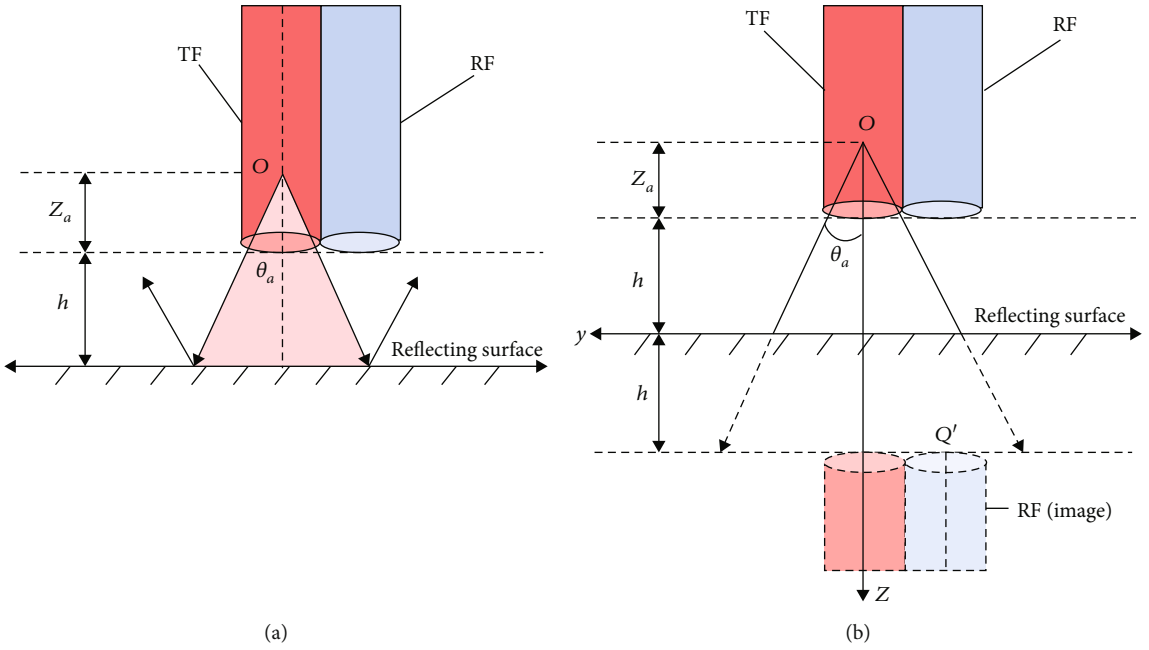

Figure 2: Illustration of the reflection of the fiber bundled probe. (a) Shaded area shows the light cone departing TF that illuminates the reflecting surface and reflected back to RF. (b) By lengthening the light cone beyond the reflecting surface, the image of the RF end can be projected to calculate the amount of light illuminated.

The main components of the optical sensor can be seen in Figure 1(b). By using a flat reflecting surface, the analysis of the displacement sensor becomes much simpler as the image of the incident light cone can be extended beyond the reflector. In Figure 2, the sketch of the reflection of light is displayed based on the geometrical optics concept, and the coordinates of the midpoint of the receiving fiber Q' are:

$$Q' \begin{cases} y = 2\omega_a, \\ z = z_a + 2h, \end{cases} \tag{1}$$

where h is the distance between the end of the probe and the reflecting surface. Based on the electromagnetic theory of paraxial Gaussian beams, it can be assumed that the optical power emitted P_E from origin at TF is a paraxial beam with a Gaussian shape which obeys an exponential law as the irradiance diminishes over the radial beam cross-section such that:

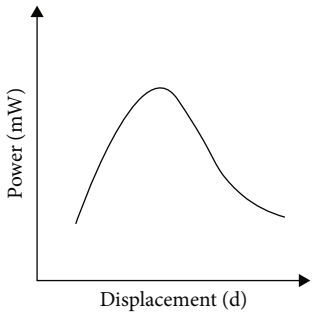

Figure 3: The power drop pattern curve by Van Etten and Van der Plaats [37].

$$I(r,z) = \frac{2P_E}{\pi\omega^2(z)} \exp\left(\frac{2r^2}{\omega^2(z)}\right), \tag{2}$$

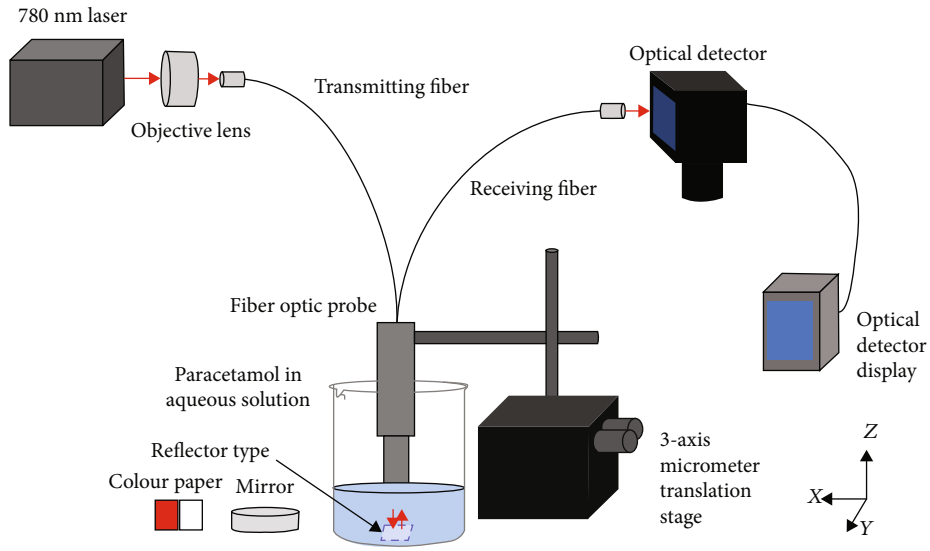

Figure 4: The experimental setup of POFDS for PCM detection. The movement of the displacement of the probe is respect to Z-axis, and there are two reflector types used in the experiment which is mirror and colour paper. Each reflector type is placed at the center bottom of the beaker.

where r is the radial coordinate, z is the longitudinal coordinate, and the radius ω is a measure of the beam width which depends on z. This can be written as [34–36]:

$$\omega(z) = \omega_0 \sqrt{1 + \left(\frac{z}{z_R}\right)^2}, \tag{3}$$

where ω_0 is the beam waist radius and z_R is the Rayleigh length and their relationship given by [34–36]:

$$\pi {\omega_0}^2 = \lambda z_R. \tag{4}$$

In the event of $z \gg z_R$ where the locations of the points are in the far-field zone, the beam would bear a resemblance to a spherical wave confined within a cone with a divergence angle θ_a of:

$$\theta_a \approx \tan\theta_a = \frac{\omega(z)}{z} = \frac{\omega_0}{z_R} = \frac{\lambda}{\pi\omega_0}, \tag{5}$$

and the irradiance function estimation yields:

$$I(r,z) = \frac{2P_E}{z^2 \pi {\theta_a}^2} \exp\left(-\frac{2r^2}{z^2{\theta_a}^2}\right). \tag{6}$$

By integrating $I(r,z)$ over the surface S_a of the fiber end, the optical power gathered by the RF can be calculated to be:

$$P(z) = \int I(r,z)dS. \tag{7}$$

The irradiance $I(r,z)$ is approximately even throughout the RF surface with area $S_a = \pi {\omega_a}^2$ which is equal to the value at Q' where $r = 2\omega_a \approx 2\theta_a z_a$. Then, the equation obtained is

$$P = IS_a = \frac{2P_E}{\zeta^2} \text{expexp}\left(-\frac{8}{\zeta^2}\right), \tag{8}$$

where

$$\zeta = \frac{z}{z_a} = 1 + \frac{2h}{z_a} = 1 + 2h_N, \tag{9}$$

and h_N is the normalized distance. By solving $dP/d\zeta = 0$, the maximum output power is achieved at $P_{\max} = P_E/4e$ when $\zeta = \sqrt{8}$, $h_N = 0.9142$. Equation (8) is thus rewritten as the normalized form of $P_N = P/P_{\max}$ as:

$$P_N = \frac{8}{\zeta^2} \text{expexp}\left(1 - \frac{8}{\zeta^2}\right). \tag{10}$$

From Figure 1(b), if $r = 0.5$ mm, $\lambda = 633$ nm, and $\omega_0 = 0.46$ mm, z_a is equal to 1141 mm. Then, $h_N = h/z_a = h/1141$ mm where h is the displacement moved in 50 μm step throughout the experiment. To calculate the sensitivity of the sensor, P_ω is differentiated with respect to h_N so that:

$$S = \frac{\partial P_N}{\partial h_N}, \tag{11}$$

to get

$$S = 2\frac{\partial P_N}{\partial \zeta} = \frac{1}{\zeta}\left(\frac{8}{\zeta^2} - 1\right) P_N(\zeta). \tag{12}$$

In this experiment, the outcome of the graph should therefore follow the Van Etten and Van der Plaats theoretical analysis in [37] where the output power is the highest after a certain displacement followed by a drop in power such as that in

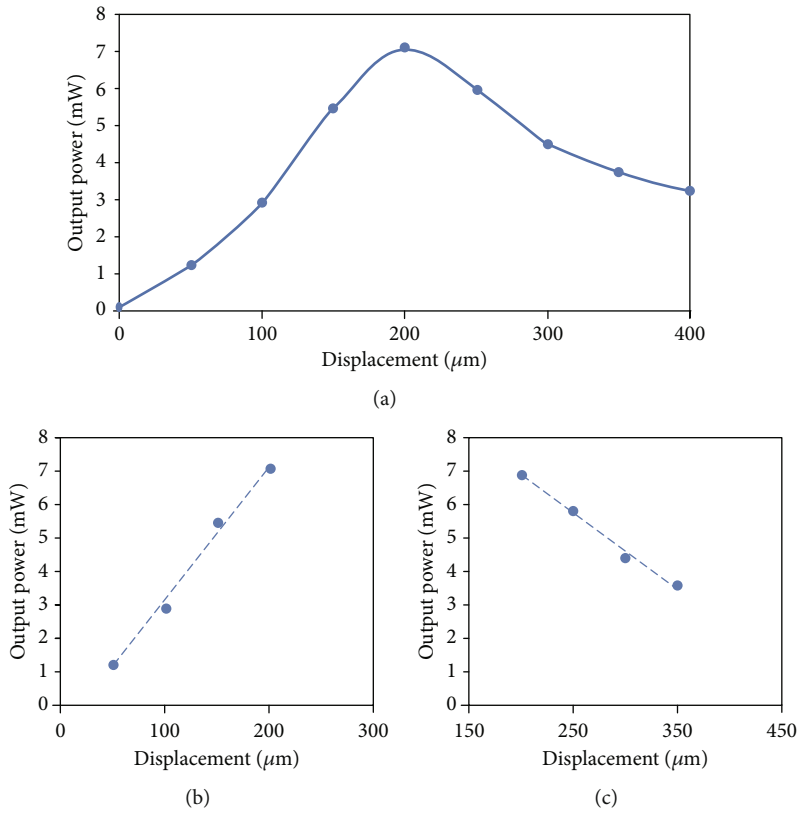

Figure 5: (a) Output power against displacement for blank solution for mirror POFDS. (b) Front slope and (c) back slope for the output power against displacement for the blank solution. The front slope and the back slope were taken from the straight line portion of the curve to measure the sensitivity of the sensor towards the changes of intensity of light against the displacement.

Figure 3. The slope of the straight-line portion of the curves defines the sensitivity of the sensor.

3. Experimental Setup

3.1. POFDS with Mirror. The experimental setup of the POFDS for the detection of PCM is given in Figure 4. The setup comprised of a 780 nm laser, a Newport M-10X objective lens with a numerical aperture (NA) of 0.25, a 2 m long Polymethyl Methacrylate (PMMA) plastic optical fiber Y -coupler, a flat cylindrical mirror, and a silicon optical detector with an optical response between 700 nm and 1800 nm. The laser source with 130 mW maximum output power projected a laser beam through the objective lens into the transmitting core. The laser beam passes through the PCM samples which then hits a Thorlabs BB03-E03 mirror located at the base of the beaker. The mirror design wavelength range is 750 nm to 1100 nm and a surface flatness of $\lambda/10$ at 632.8 nm over a clear aperture. The intensity of the laser reflected from the mirror was collected by 16 receiving cores with NAs of 0.5, core refractive indices of 1.492, and cladding refractive indices of 1.402. The output power was measured by an optical detector connected to a digital power meter display.

The coupler probe was mounted on a 3-axis micrometer translation stage fixed on a vibration free table. The displacement was determined by withdrawing the coupler probe from the starting point, where the mirror and the probe were nearly making contact with each other. By rotating the Z-axis translational control knob, the position of the probe from the mirror was made to increase by 50 μm for each step. To zero the Z-axis knob, a universal micrometer spanner wrench is used to ensure the position of the zero scale is placed precisely. The increment calibration on Z-axis is done by comparing each step to a digital vernier caliper of 10 μm resolution to ensure the increment of the knob is accurate to the scale. The concentrations of PCM used were varied from 5 ppm to 45 ppm, and all measurements were done at room temperature under the atmospheric pressure.

Table 2: Summary of the sensor response for the blank solution using mirror POFDS.

Front slope		Back slope	
Sensitivity (mW/μm)	Linearity (%)	Sensitivity (mW/μm)	Linearity (%)
0.0403	>99	-0.023	>99

By employing an OBIS Coherent laser, a potential source of error in the experiment could be reduced as this laser ensures a stable output power with little to no fluctuations. To avoid interference from other stray light sources, the experiment was done in a closed container. To reduce any possible physical vibrations, the experiment was conducted on a vibration-free table manufactured by Thorlabs. The data and analysis was done by using a normal data analysis software.

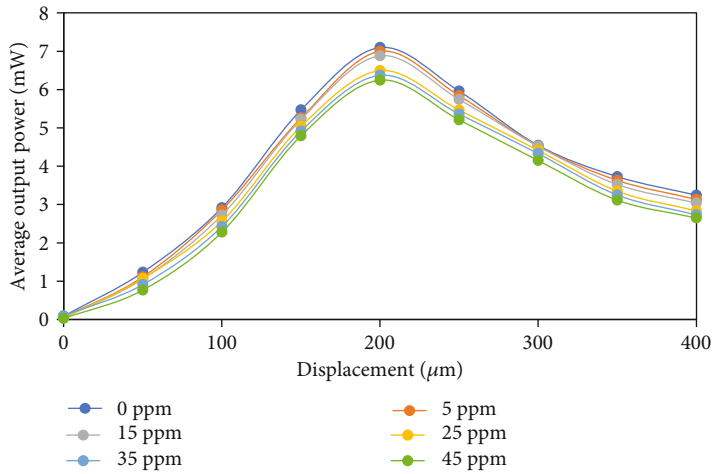

Figure 6: Average output power against displacement at different concentration of PCM for mirror POFDS.

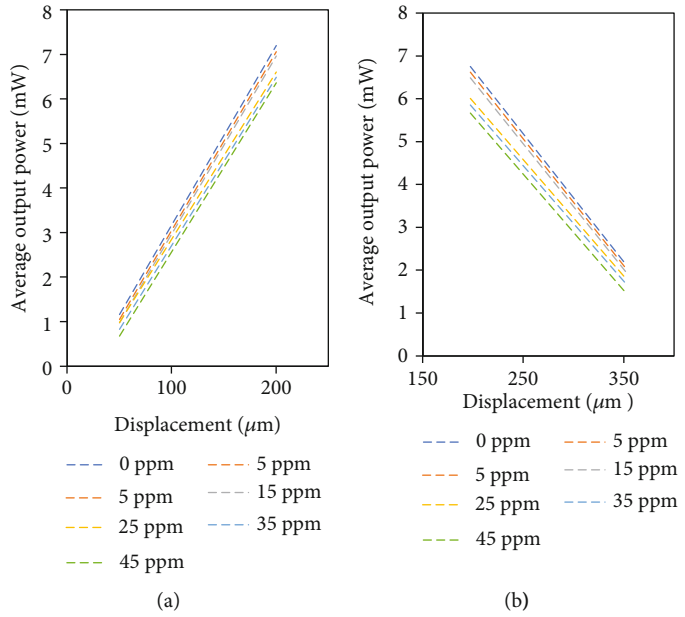

Figure 7: (a) Front slope and (b) back slope at different concentrations of PCM using mirror POFDS.

3.2. POFDS without Mirror. The experiment was then repeated using a similar approach but with the reflector changed to coloured paper. In Figure 4, the colours chosen for the reflector were white and red to reflect only specific wavelengths [38]. A 2 cm × 3 cm 80 gsm white and red Mirrorkote® waterproof adhesive paper is used in this experiment. The displacement of the probe was achieved in the same manner as before by fixing it onto the Thorlabs micrometer translation stage, and the direction of the movement is controlled via the Z-axis with the increment of 50 μm for each step.

3.3. Preparations of the Paracetamol (Acetaminophen) Solution. The PCM powder was purchased from Sigma-Aldrich (Darmstadt, Germany). The solutions ranged from 5 ppm to 45 ppm, and nine replicates were done for each concentration. Each replicate is prepared by weighing the PCM powder and then carefully added into a 100 ml volumetric flask of distilled water at room temperature (25°C). The solutions were dissolved by gently stirred until no clumps or any large particle could be observed. A new weighed quantity of PCM in 100 ml of distilled water is done for each replication at each concentration from 5 ppm to 45 ppm. The solution then was poured into a 100 ml beaker to be detected by the sensor.

4. Results and Discussion

4.1. POFDS with Mirror. A response was first obtained in a distilled water to provide an insight of the pattern that should be observed. The increment of the probe is set from 0 μm to 400 μm which is sufficient to correspond to the output power of the laser. The intensity of the reflected output power shows no change after the increment is increased. In Figure 5(a), the experimental curve obtained shows a good sensor response with a gradual increase in the output power for the front

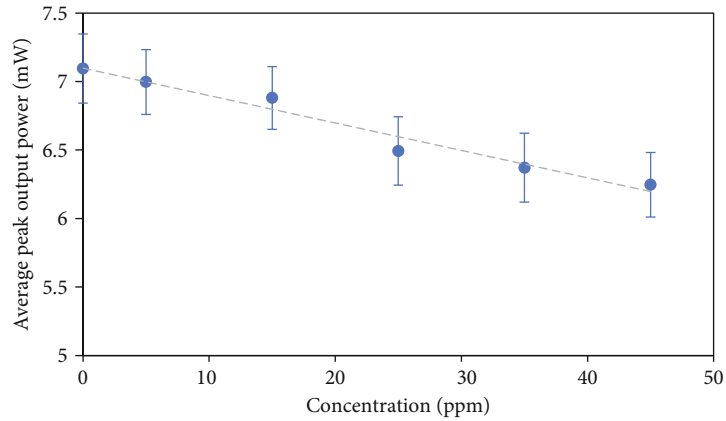

Figure 8: Average peak output power vs. concentration of PCM.

Table 3: Summary of the features of the sensor for each red and white reflector.

Colour of reflector	Paracetamol concentration (ppm)	Peak output power (mW)	Front slope		Back slope	
			Sensitivity (mW/mm)	Linearity (%)	Sensitivity (mW/mm)	Linearity (%)
Red	5	0.142	0.0006	98	-0.0002	99
	15	0.136	0.0006	98	-0.0002	99
	25	0.132	0.0006	99	-0.0001	99
	35	0.129	0.0005	98	-0.0001	99
	45	0.126	0.0006	98	-0.0001	99
White	5	0.175	0.0006	97	-0.0003	99
	15	0.166	0.0006	97	-0.0002	99
	25	0.161	0.0006	97	-0.0002	99
	35	0.152	0.0005	97	-0.0002	99
	45	0.145	0.0005	95	-0.0002	99

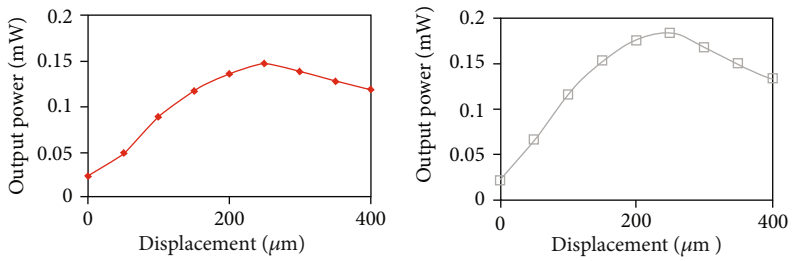

Figure 9: Experimental curve of (a) red colour paper and (b) white colour paper for output power against displacement for blank solution.

slope. Meanwhile, the back slope is inversely proportional to the distance from the source of the reflected output power. The reflected output power was zero at 0 μm displacement because the tip of the probe was so close to the mirror surface that no light was reflected back to RF. As the displacement increased, RF started to collect the light reflected from the mirror, and the output power increased to the maximum value. The output power peak in accordance with the reflected cone of light is illustrated in Figure 2 and can be seen to have overlapped most of the core area of RF [39]. As the displacement increased, specifically from 250 μm to 400 μm, the output power decreased because the size of the

Table 4: Summary of the features of the sensor using mirror as reflector.

Paracetamol concentration (ppm)	Front slope		Back slope	
	Sensitivity (mW/μm)	Linearity (%)	Sensitivity (mW/μm)	Linearity (%)
5	0.0401	99	-0.0228	99
15	0.0399	99	-0.0227	99
25	0.0375	99	-0.021	99
35	0.0377	99	-0.0209	99
45	0.0379	99	-0.021	99

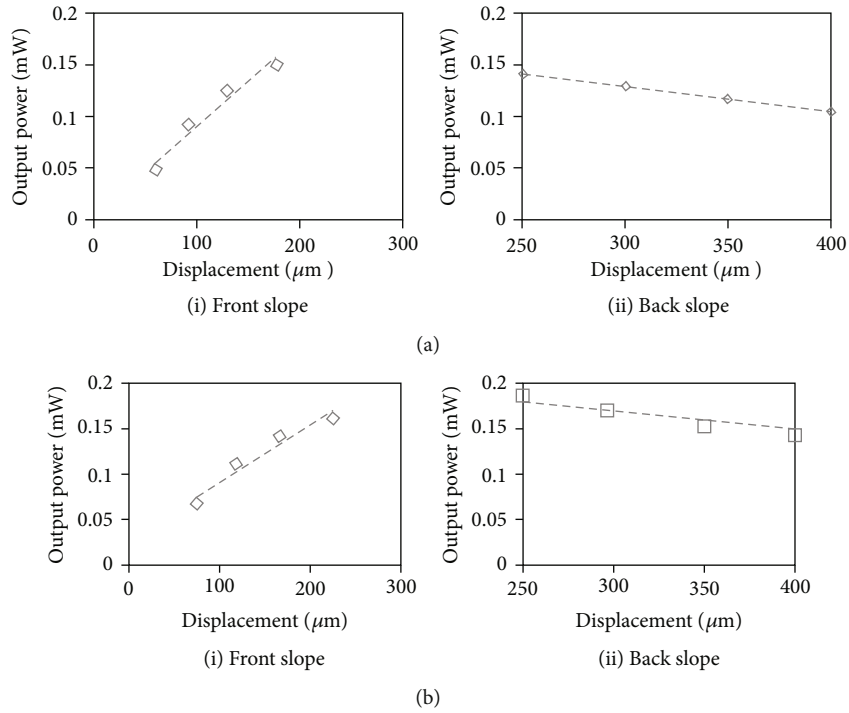

Figure 10: Linearity graph for (a) red and (b) white reflector of the output power against displacement for blank solution.

light cone became very large. As a result, the intensity of reflected laser collected by the receiving fiber started to reduce. This pattern would thus also be observed for the samples that contain the analytes of interest, albeit at different output power values.

In Figures 5(b) and 5(c), the linearity attained from the front and the back slopes for the blank solution was 99% and indicated a good basis results to compare with other data obtained. The front slope and the back slope had a sensitivity of 0.0403 mW/μm and 0.023 mW/μm, respectively. These slopes indicate the sensitivity of the sensor where the straight line portion of the curve is plotted to create a linear graph to analyse the sensors' sensitivity [37]. From the data, the sensor was able to detect a high output power reflected from the mirror up to 1 μm of the displacement. The responses from the sensor are summarized in Table 2.

The signal obtained from the probe in the presence of various concentrations of PCM was plotted against the displacement as shown in Figure 6. The pattern of the curves shown in Figure 6 follows a similar trend to the response obtained in the blank solution which confirms that the results follow the inverse square relationship where the intensity of the reflected laser is inversely proportional to the distance of the source. Therefore, it is also plausible to resolve and analyse the data in a similar approach when treating the data recorded in the blank solution. The results are also seen to follow the rule of thumb [40] of the displacement sensor.

The highest sensitivity was obtained for a PCM solution at 5 ppm as 0.0401 mW/μm for the front slope and 0.023 mW/μm for the back slope. The spectrum obtained for 5 ppm PCM solution also showed the highest output power among the measured spectra. This could due to the concentration of the PCM in the solution being fairly low, and therefore, most of the light emitted by the probe and reflected by the mirror does not scatter due to the lower amount of PCM particles in the laser trajectory. Thus, almost all of the reflected laser is collected by the receiving fiber. Meanwhile, the spectrum recorded for the PCM solution at 45 ppm had a sensitivity of 0.0379 mW/μm and 0.021 mW/μm for the front and back slopes, respectively. It showed the lowest output power as compared to other spectra because most of the laser was scattered by the large amount of PCM molecules. Therefore, the lower the concentration of the analyte, the higher the sensitivity of the sensor and the larger the output power in the given range of displacement.

The sensitivity of the sensor with respect to the changes of output power over the displacement for the front and the back slopes for each curve is given in Figure 7. The lower PCM concentration renders a greater sensitivity of the sensor to determine the PCM concentration. Linear relationships were observed for the graphs of the output power versus the displacement for both the front and back slopes for each concentration while most of it achieved a linearity of 99%. The performance of the sensor is summarized in Table 2.

Figure 8 exhibits a linear relationship between the average peak output power and the concentration of PCM. From the analysis, the sensor was capable of sensing any given concentration within the range from 0 ppm to 45 ppm due to the linearity of more than 96%. This enables the sensor to provide readings at a resolution of 0.02 mW/ppm which indicates that the sensor has high sensitivity towards the PCM in the solution. The highest peak output power and the lowest peak output power obtained are 6.996 mW and 6.246 mW for 5 ppm and 45 ppm, respectively. Significant shifts in the peak output power were observed for each concentration of the PCM, and this implies that the sensor could detect small

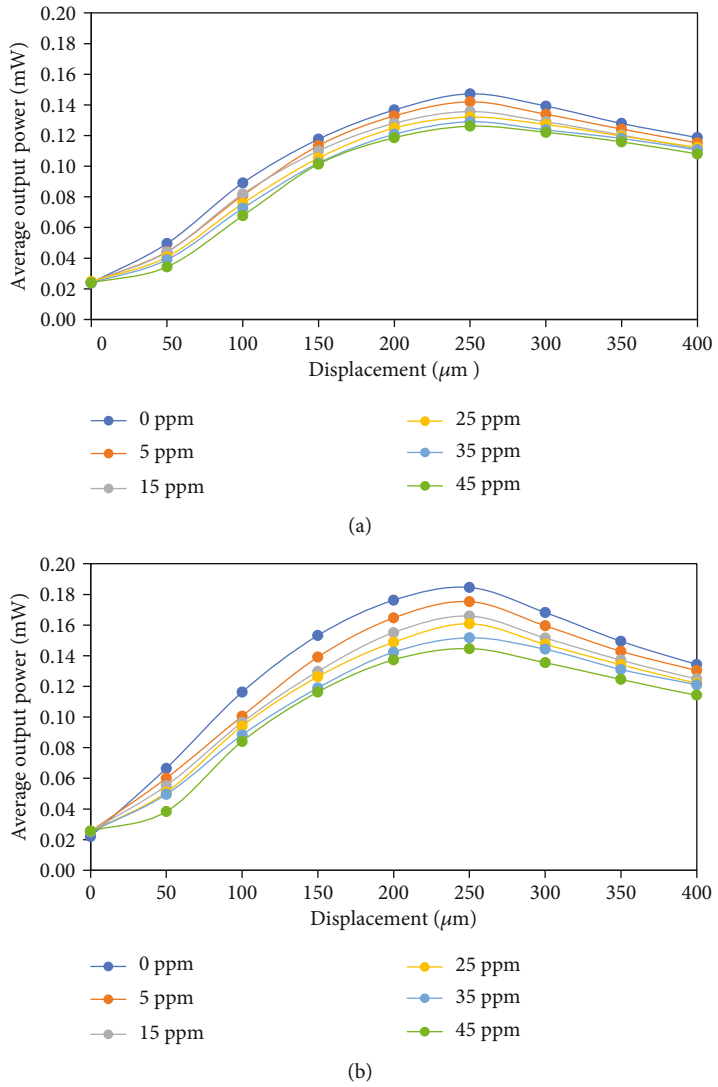

Figure 11: The average output power against displacement for (a) red and (b) white reflector at different concentrations of PCM.

changes in the concentration of analytes. The error bar in the graph indicates that value of the peak output power in each replicate is spread in a small standard deviation (SD) value around the mean value. The characteristic of this sensor is summarized in Table 3.

The higher output power is closely related to the larger amount of reflected laser picked up by RF. This is caused by the low refractive index in the solution [41], and thus, a higher intensity laser transmission could be emitted through the sample. The increasing PCM quantity added into the solution increases the refractive index as this allows the laser to further disperse into the solution instead of being reflected to RF. Basically, higher refractive index material has a lower refraction angle [42] that causes the decrease in the peak output power as the concentration increases. From the data, it is very interesting to note that each concentration of the tested PCM has a different value of peak output power with different intensity. This means that the sensor has the ability to reiterate the similar measurement of the intensity based signal for the same concentration.

Table 5: Summary of the capabilities of the sensor with red and white reflector for blank solution.

Colour of reflector	Front slope		Back slope	
	Sensitivity (mW/μm)	Linearity (%)	Sensitivity (mW/μm)	Linearity (%)
Red	0.0006	>98	-0.0002	>99
White	0.0007	>95	-0.0003	>98

4.2. POFDS without Mirror. The experiment was then continued with the reflector now changed to the red and white coloured paper. These colours were chosen based on the previous work by the authors in the colour detection using the fiber optic displacement sensor [43]. From the previous research, red and white colour paper reflects the most of the projected light and projected a very stable outcome in terms of output power of the intensity of the reflected light. This is because different colour can absorb and reflect different wavelength [44]. Thus, both of these coloured paper reflectors are believed to have the capabilities of replacing

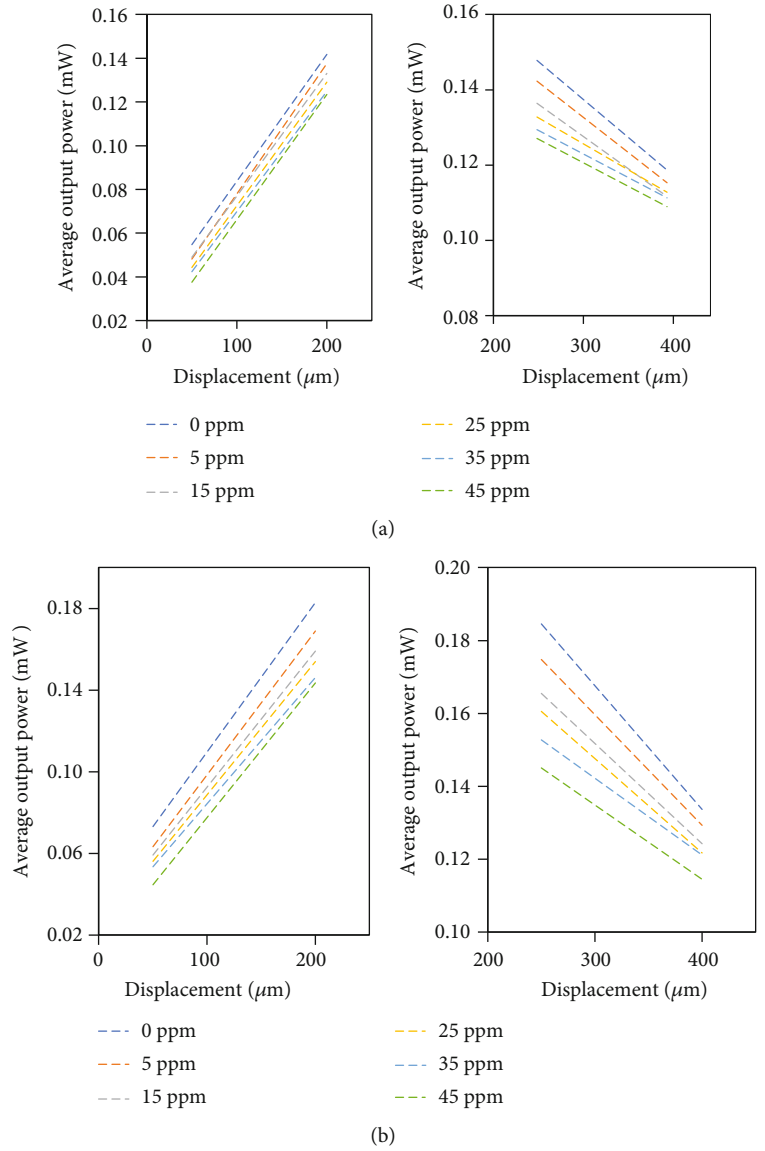

Figure 12: Linearity graph for (a) red and (b) white reflector of the average output power against displacement for different concentration of PCM.

the mirror to compensate the amount of stray light that can affect the reading of the sensor. Due to low concentration of PCM to be tested, the amount of the displacement of the probe is limited to 400 μm which correspond to the output power of the laser. No change in the intensity of the reflected output power after the displacement exceeded this range has been detected. Based on Figure 9, the response for both reflectors were tested in a distilled water to give an overview of the pattern of the curve that should be observed. Both colours provide good experimental curves with a gradual increase of the front slope and gradual decrease of the back slope in accordance to the inverse square relationship curve. At 0 μm displacement, the output power was close to 0 mW because the gap between the probe and the reflector was very near, causing almost no reflected laser to be collected by RF. When the displacement was increased, the overlap between the reflected cone of light with RF was enlarged [39]. Hence, the output power started to rise to reach its maximum value at 250 μm displacement. After this, the output power decreased with further increment of the displacement as RF was no longer able to effectively pick up the reflected laser and TF starting to disperse even more and losing its intensity.

Table 6: Comparison of attributes of the paracetamol POFDS for each reflector.

Reflector	Concentration range (ppm)	Sensitivity (mW/ppm)	Linearity (%)
Red colour paper	5-45	0.0004	95
White colour paper	5-45	0.0008	98
Mirror	5-45	0.02	95

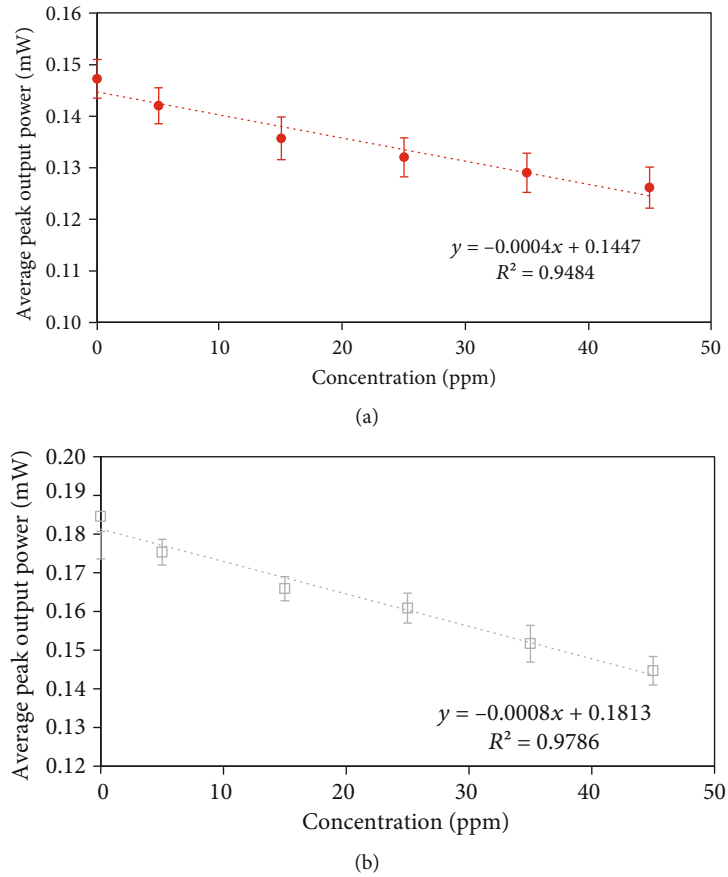

Figure 13: Linear relationship of (a) red colour paper and (b) white colour paper for average peak output power against concentration of PCM.

Thus, this experimental curve was used as the benchmark for all samples.

Table 4 shows that the linearity for both front slope and the back slope of each colour was greater than 95%. This proves that this sensor has a great base data to be evaluated with other samples. Figure 10 shows that the white reflector has a greater sensitivity on the front slope as compared to the red reflector with 0.0007 mW/μm and 0.0006 mW/μm, respectively. This shows that the sensor can measure the intensity of the output power in displacement increments of 1 μm. From the experimental curve, all samples should follow the pattern of the blank solution.

The response of the sensor for both reflectors towards the changes of the PCM concentration is plotted in Figure 11 against the displacement of the sensor. All curves for both red and white coloured papers reproduce the same pattern as set by the blank solution. The highest and the lowest peak output power set by red colour paper was 0.147 mW and 0.126 mW, respectively. Meanwhile, for the white coloured paper, the highest peak output power plotted was 0.185 mW while the lowest peak output power was 0.145 mW for 0 ppm and 45 ppm, respectively. The higher peak output power was caused by the lower refractive index of the solution which allowed more reflected laser light to be collected by RF. Greater amounts of PCM make the solution more concentrated and thus have a higher refractive index [41], in turn lowering the peak output power. This is because whenever the laser hits the sample, it will disperse significantly, and therefore, a lower laser intensity can be collected by RF.

From Figure 11, each PCM concentration shows a significant difference in the maximum output power. This proves that the sensor can differentiate between different concentrations of PCM and therefore indicates that even when the reflector has been changed from a mirror to just coloured paper, the sensor still functions well to detect the concentration of solution. In Table 5, the highest front slope sensitivity of the sensor towards the changes of output power over the displacement was gained by the white reflector at 0.0007 mW/μm, and the lowest sensitivity was plotted by the red reflector at 0.0005 mW/μm. From Figure 12, both slopes for each colour had a linearity greater than 95% which proves that the sensor is highly reliable.

Table 6 displays the variation of peak output power with different concentrations of PCM for red and white reflector. The highest peak output power was 0.175 mW from the white reflector, and the lowest peak output power was 0.126 mW from the red reflector. The amount of the output power signifies the intensity of the laser passing through and thus indicates that the white colour paper can reflect higher laser power in comparison to the red colour paper. Furthermore, the tendency of laser scattering whenever it hits

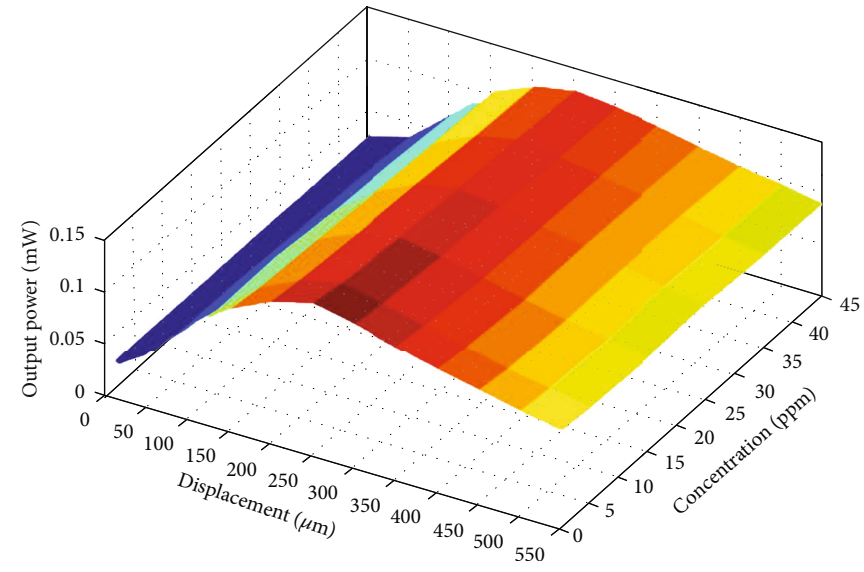

(i)

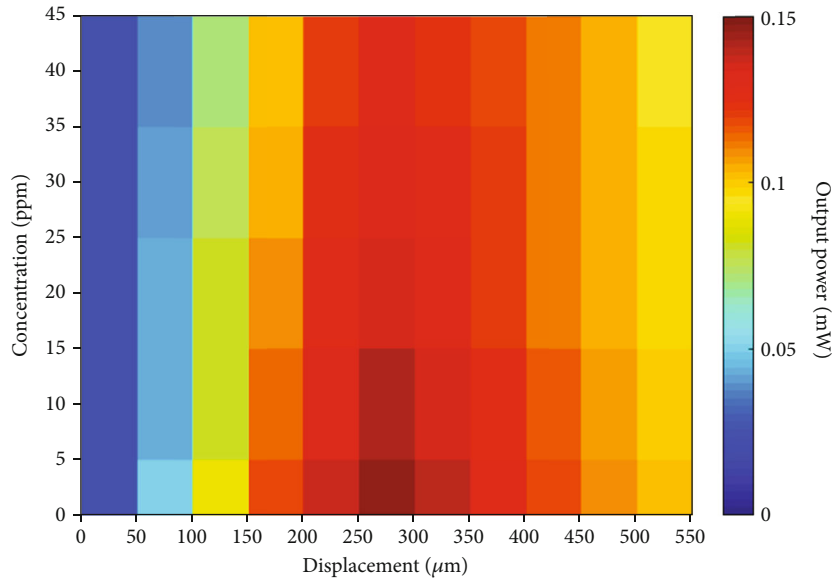

(ii)

(a) Red reflector

Figure 14: Continued.

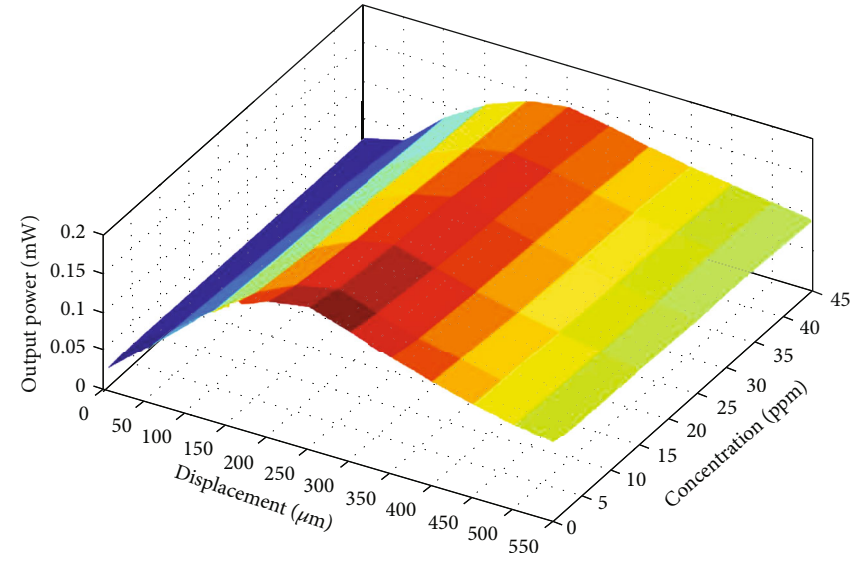

(i)

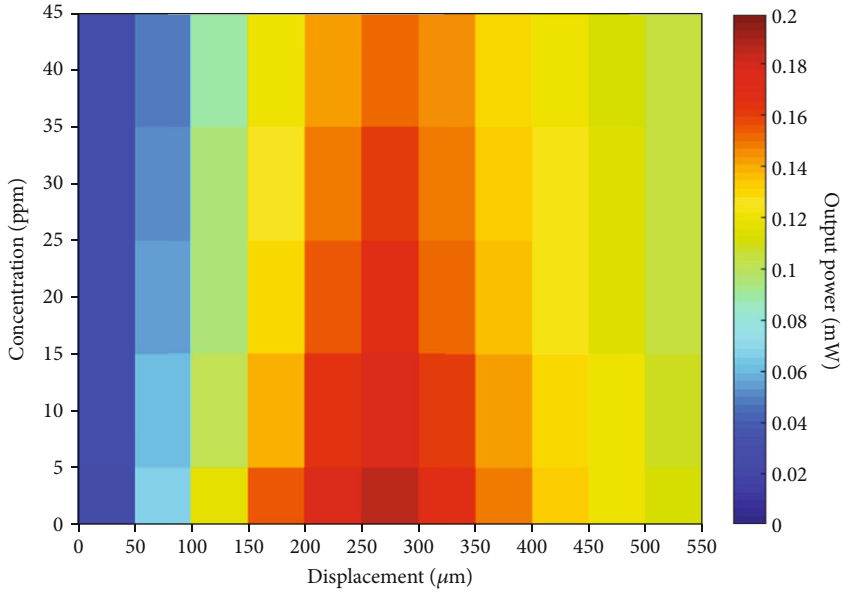

(ii)

(b) White reflector

Figure 14: Continued.

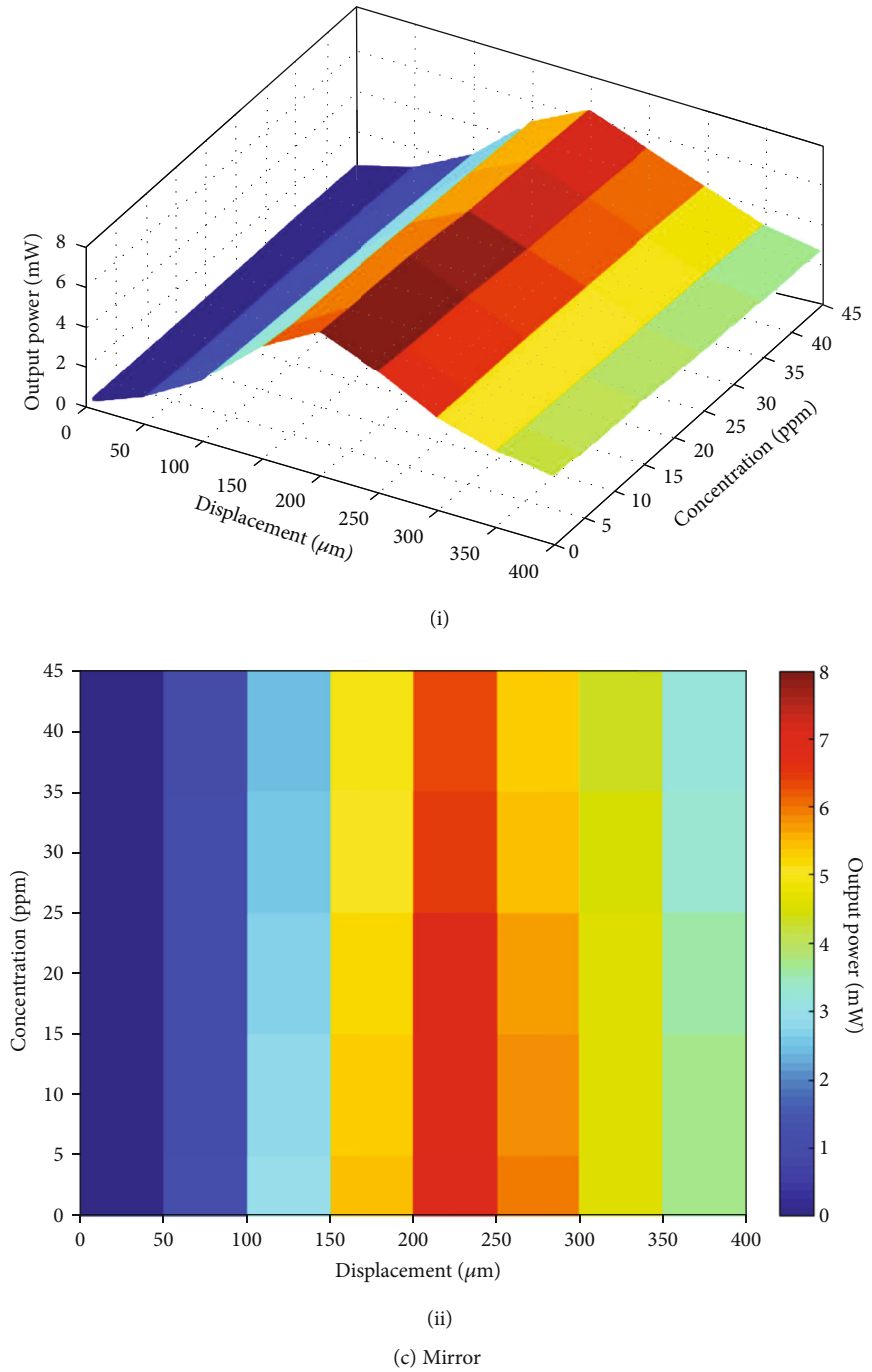

FIGURE 14: The (i) 3D model intensity graph and (ii) graph of the intensity of output power for each type of reflector with different concentrations of paracetamol.

the sample is decreases when the concentration of PCM is low. More concentrated solution causes higher refractive index, and the laser tends to scatter more in a higher refractive index solution. It is quite clear that the higher the concentration of PCM, the lower the intensity of the reflected laser, due to less laser light being transmitted to RF because of higher scattering of laser and thus a lower output power detected by the optical detector.

From Figure 13, the sensor was capable of sensing up to 0.0008 mW/ppm for the white reflector and 0.0004 mW/ppm for the red reflector, respectively. The sensor was very reliable and could detect small changes in the concentration of the solutions because significant changes in the peak output power could be observed for each PCM concentration with more than 95% of linearity. The error bars from both graphs also display a small spread of SD value around the mean. Therefore, both the red and white reflector could also be used to identify unknown PCM concentrations at certain displacements. The performance of this sensor using these reflectors is summarized in Table 3.

From Figure 14, the highest sensitivity among all reflectors is undoubtedly the mirror at 0.02 mW/ppm while the lowest was the red coloured paper at 0.0004 mW/ppm. However, the white coloured paper returned a significant result with a sensitivity of 0.0008 mW/ppm towards different PCM concentrations and showed good feedback from the sensor. With a 98% linearity, the result proved that the sensor was very reliable when using the white coloured paper as a reflector. From the error bar in Figures 13(a) and 13(b), it can be seen that the coloured paper had a narrower spread compared to the mirror in Figure 8 indicating that the peak output power is accumulated near the mean. Thus, concise data is established to note that the red and white reflector is capable of detecting different concentration of PCM in the distilled water with the addition of steady output power from each replicate. It shows that the coloured paper reflector managed to get a stable and consistent outcome as compared to the mirror. The coloured paper reflector could compensate for stray light from the surroundings unlike the mirror which had the tendency to reflect all lights, including those that would affect the reading of the optical detector. From the comparison table, the red and white reflectors had the ability to recreate similar detection for PCM concentrations by using as intensity-based PODFS.

5. Conclusion

The detection of the PCM concentrations in an aqueous solution was proposed and demonstrated using a PODFS. The sensor displayed good patterns for each reflector curve with a gradual increase in the front slope and decrease in the back slope similar to the inverse square law relationship. For the PODFS using the mirror reflector, the sensitivity of the sensor towards the changes of output power over the displacement was 0.0403 mW/μm for the front slope and 0.023 mW/μm for the back slope with more than 99% of linearity. The highest output recorded was 6.996 mW for a PCM concentration of 5 ppm with the sensitivity of 3.603 mW/μm for front slope and 1.987 mW/μm for back slope. Meanwhile, the lowest output power was 6.246 mW for a PCM concentration of 45 ppm with the sensitivity of the front and back slope at 3.312 mW/μm and 1.879 mW/μm, respectively. For the non-mirror reflectors, the sensitivity of the sensor with the changes of output power over the displacement taken was 0.0006 mW/μm for front slope and 0.0002 mW/μm for back slope of the red reflector. In the meantime, the white reflector had a sensitivity of 0.0007 mW/μm and 0.0003 mW/μm for the front and the back slope, respectively. Each reflector had a linearity of more than 95% and sensor sensitivity with respect to the output power against different PCM concentrations at 0.0004 mW/ppm, 0.0008 mW/ppm, and 0.02 mW/ppm for the red coloured paper, white coloured paper, and mirror. This outcome would make this sensor highly appealing for the pharmaceutical industries to establish an easy and accurate approach to detect PCM using POFDS in order to work rapidly, effectively, cheaply, and with good accuracy. The lengthy predetection extraction and long-running processes in traditional sensors can be eschewed when it comes to testing huge quantities of samples for the presence of PCM, especially in healthcare, aquatic environments, wastewater, and drinking water in many parts of the world. Thus, this experiment concurs that this mirrorless PODFS shows significant potential as a PCM detection device as it is simple, fast, and has a low production cost, with the possibility of being a widely used sensor in the future.

Data Availability

The graphs and table data used to support the findings of this study are included within the article.

Conflicts of Interest

The authors declare no competing interests.

Acknowledgments

We would like to thank Ministry of Education of Malaysia for providing the funding for this work under the grant FRGS (FP044-2014A), the HIR Grant (UM.C/625/1/HIR/MoHE/SC/29/01), the International Islamic University Malaysia RMC Grant 2020 (RMCG20-038-0038), and the SPIE Education Outreach Grants Program (2020).

References

[1] L. Liu, H. Lv, C. Wang, Z. Ao, and G. Wang, "Fabrication of the protonated graphitic carbon nitride nanosheets as enhanced electrochemical sensing platforms for hydrogen peroxide and paracetamol detection," *Electrochimica Acta*, vol. 206, pp. 259–269, 2016.

[2] R. M. de Carvalho, R. S. Freire, S. Rath, and L. T. Kubota, "Effects of EDTA on signal stability during electrochemical detection of acetaminophen," *Journal of Pharmaceutical and Biomedical Analysis*, vol. 34, no. 5, pp. 871–878, 2004.

[3] R. Kachoosangi, G. Wildgoose, and R. Compton, "Sensitive adsorptive stripping voltammetric determination of paracetamol at multiwalled carbon nanotube modified basal plane pyrolytic graphite electrode," *Analytica Chimica Acta*, vol. 618, no. 1, pp. 54–60, 2008.

[4] R. Goyal, V. Gupta, M. Oyama, and N. Bachheti, "Differential pulse voltammetric determination of paracetamol at nanogold modified indium tin oxide electrode," *Electrochemistry Communications*, vol. 7, no. 8, pp. 803–807, 2005.

[5] S. Heitmeier and G. Blaschke, "Direct determination of paracetamol and its metabolites in urine and serum by capillary electrophoresis with ultraviolet and mass spectrometric detection," *Journal of Chromatography B: Biomedical Sciences and Applications*, vol. 721, no. 1, pp. 93–108, 1999.

[6] M. Li and L. Jing, "Electrochemical behavior of acetaminophen and its detection on the PANI-MWCNTs composite modified electrode," *Electrochimica Acta*, vol. 52, no. 9, pp. 3250–3257, 2007.

[7] H. M. Moghaddam, "Electrocatalytic determination of carbidopa and acetaminophen using a modified carbon nanotube paste electrode," *International Journal of Electrochemical Science*, vol. 6, no. 12, pp. 6557–6566, 2011.

[8] H. Filik, G. Çetintaş, A. Aslihan Avan, S. N. Koç, and I. Boz, "Electrochemical sensing of acetaminophen on electrochemically reduced graphene oxide-nafion composite film modified

electrode," *International Journal of Electrochemical Science*, vol. 8, no. 4, pp. 5724–5737, 2013.

[9] W. M. Lee, "Acetaminophen and the U.S. acute liver failure study group: lowering the risks of hepatic failure," *Hepatology*, vol. 40, no. 1, pp. 6–9, 2004.

[10] MedicineWise, "Rates of paracetamol overdose continue to rise in Australia," *NPS Med*, 2019.

[11] C. Bourdeaux and J. Bewley, "Death from paracetamol overdose despite appropriate treatment with N-acetylcysteine," *Emergency Medicine Journal*, vol. 24, no. 5, pp. e31–e34, 2007.

[12] S. Wu, L. Zhang, and J. Chen, "Paracetamol in the environment and its degradation by microorganisms," *Applied Microbiology and Biotechnology*, vol. 96, no. 4, pp. 875–884, 2012.

[13] D. Šatínský, I. Neto, P. Solich et al., "Sequential injection chromatographic determination of paracetamol, caffeine, and acetylsalicylic acid in pharmaceutical tablets," *Journal of Separation Science*, vol. 27, no. 7-8, pp. 529–536, 2004.

[14] E. Llorent-Martínez, D. Šatínský, P. Solich, P. Ortega-Barrales, and A. Molina-Díaz, "Fluorimetric SIA optosensing in pharmaceutical analysis: determination of paracetamol," *Journal of Pharmaceutical and Biomedical Analysis*, vol. 45, no. 2, pp. 318–321, 2007.

[15] M. Yasin, H. Ahmad, K. Thambiratnam, A. A. Jasim, S. W. Phang, and S. W. Harun, "Design of multimode tapered fibre sensor for glucose detection," *Optoelectronics and Advanced Materials*, vol. 7, no. 5–6, pp. 371–376, 2013.

[16] M. M. Huber, A. GÖbel, A. Joss et al., "Oxidation of pharmaceuticals during ozonation of municipal wastewater effluents: a pilot study," *Environmental Science & Technology*, vol. 39, no. 11, pp. 4290–4299, 2005.

[17] X. Kang, J. Wang, H. Wu, J. Liu, I. A. Aksay, and Y. Lin, "A graphene-based electrochemical sensor for sensitive detection of paracetamol," *Talanta*, vol. 81, no. 3, pp. 754–759, 2010.

[18] Y. Fan, J. Liu, H. Lu, and Q. Zhang, "Electrochemical behavior and voltammetric determination of paracetamol on Nafion/-TiO_2-graphene modified glassy carbon electrode," *Colloids Surfaces B Biointerfaces*, vol. 85, no. 2, pp. 289–292, 2011.

[19] Y. Teng, L. Fan, Y. Dai, M. Zhong, X. Lu, and X. Kan, "Electrochemical sensor for paracetamol recognition and detection based on catalytic and imprinted composite film," *Biosensors & Bioelectronics*, vol. 71, pp. 137–142, 2015.

[20] L. Shiroma, M. Santhiago, A. L. Gobbi, and L. T. Kubota, "Separation and electrochemical detection of paracetamol and 4-aminophenol in a paper-based microfluidic device," *Analytica Chimica Acta*, vol. 725, pp. 44–50, 2012.

[21] D. Easwaramoorthy, Y. Yu, and H. Huang, "Chemiluminescence detection of paracetamol by a luminol-permanganate based reaction," *Analytica Chimica Acta*, vol. 439, no. 1, pp. 95–100, 2001.

[22] S. Zhao, W. Bai, H. Yuan, and D. Xiao, "Detection of paracetamol by capillary electrophoresis with chemiluminescence detection," *Analytica Chimica Acta*, vol. 559, no. 2, pp. 195–199, 2006.

[23] M. Yasin, S. Soelistiono, Y. Y. Yhuwana et al., "Intensity based optical fiber sensors for calcium detection," *Journal of Optoelectronics and Advanced Materials-Rapid Communications*, vol. 9, no. 9–10, pp. 1185–1189, 2015.

[24] N. Hida, N. Bidin, M. Abdullah, and M. Yasin, "Fiber optic displacement sensor for honey purity detection in distilled water," *Optoelectronics and Advanced Materials*, vol. 7, no. 7–8, pp. 565–568, 2013.

[25] M. Budiyanto, S. W. Harun, and M. Yasin, "Fiber Optic Displacement Sensor for Measuring Cholesterol Concentration," *Sensors & Transducers*, vol. 217, no. 11, pp. 45–48, 2017.

[26] M. Yasin, N. Irawati, A. H. Zaidan et al., "Fiber bundle sensor for detection of formaldehyde concentration in fish," *Optical Fiber Technology*, vol. 52, 2019.

[27] H. A. Rahman, S. W. Harun, M. Yasin, and H. Ahmad, "Fiber-optic salinity sensor using fiber-optic displacement measurement with flat and concave mirror," *IEEE Journal of Selected Topics in Quantum Electronics*, vol. 18, no. 5, pp. 1529–1533, 2012.

[28] M. Yasin, S. W. Harun, C. F. Tan, S. W. Phang, and H. Ahmad, "Fiber optic chemical sensor using fiber coupler probe based on intensity modulation for alcohol detection," *Microwave and Optical Technology Letters*, vol. 53, no. 8, 2011.

[29] H. A. Rahman, S. W. Harun, M. Yasin, and H. Ahmad, "Fiber-optic salinity sensor using fiber-optic displacement measurement with flat and concave mirror," *IEEE Journal of Selected Topics in Quantum Electronics*, vol. 18, no. 5, pp. 1529–1533, 2012.

[30] H. A. Rahman, S. W. Harun, M. Yasin, and H. Ahmad, "Fiber optic salinity sensor using beam-through technique," *Optik - International Journal for Light and Electron Optics*, vol. 124, no. 8, pp. 679–681, 2013.

[31] K.-C. Liao, S.-C. Chang, C.-Y. Chiu, and Y.-H. Chou, "Acute response in vivo of a fiber-optic sensor for continuous glucose monitoring from canine studies on point accuracy," *Sensors*, vol. 10, no. 8, pp. 7789–7802, 2010.

[32] S. W. Phang, H. Z. Yang, S. W. Harun, H. Arof, and H. Ahmad, "Simple fiber optic sensor based on tapered fiber for aliphatic alcohol detection," *Journal of Optoelectronics and Advanced Materials*, vol. 13, no. 5–6, pp. 604–608, 2009.

[33] J. B. Faria, "A theoretical analysis of the bifurcated fiber bundle displacement sensor," *IEEE Transactions on Instrumentation and Measurement*, vol. 47, no. 3, pp. 742–747, 1998.

[34] J. Faria, "Optics - Fundamentals and Applications," *Editorial Presence*, vol. 1, 1995.

[35] B. Saleh and M. Teich, "*Fundamentals of Photonics*," *John Wiley & Sons*, vol. 193, 1999.

[36] A. Siegman, "No title," *Lasers*, vol. 1, 1986.

[37] E. W. Van and D. P. J. Van, *Fundamentals of Optical Fiber Communications*, Prentice-Hall., no. Prentice-Hall international series in optoelectronics, London, 1991.

[38] C. Deziel, "Which colors reflect more light?," 2020, https://sciencing.com/colors-reflect-light-8398645.html.

[39] M. Yasin, S. W. Harun, H. A. Abdul-Rashid, Kusminarto, Karyono, and H. Ahmad, "The performance of a fiber optic displacement sensor for different types of probes and targets," *Laser Physics Letters*, vol. 5, no. 1, pp. 55–58, 2008.

[40] P. Regtien and E. Dertien, "Capacitive sensors," *Sensors for Mechatronics*, vol. 2, 2018.

[41] W. M. b. M. Yunus and A. b. A. Rahman, "Refractive index of solutions at high concentrations," *Applied Optics*, vol. 27, no. 16, pp. 3341–3343, 1988.

[42] B. W. Grange, W. H. Stevenson, and R. Viskanta, "Refractive index of liquid solutions at low temperatures: an accurate measurement," *Applied Optics*, vol. 2, 1975.

[43] M. F. M. Azri, M. Z. Zulkifli, F. D. Muhammad et al., "Color detection usingnon-targetreflectivity plastic optical fiber displacement sensor," *Microwave and Optical Technology Letters*, vol. 62, no. 11, pp. 3640–3644, 2020.

[44] J. P. Straley and S. A. Shafer, "Physics of light," 2000, http://www.pa.uky.edu/~sciworks/light/preview/color4aa.htm#:~:text=One consequence of the fact, reflect most of the wavelengths.